LONGITUDINAL ELECTRON-BEAM PUMPED RARE GAS-HALIDE EXCIMER LASERS*

W.L. Wilson, Jr. and F.K. Tittel,
Electrical Engineering Department
Rice University, Houston TX 77251

W. Walter and R. Sauerbrey
Physikalisches Institut der Universitat Wurzburg,
D-8700 Wurzburg, F. R. Germany

and

G. Marowsky
Max-Planck Institut fur biophysikalische Chemie
D-3400 Gottingen, F.R. Germany

Abstract

Longitudinal electron beam pumping of excimer lasers in a head-on configuration was investigated. Laser experiments on the B->X and C->A transition of XeF, as well as experiments with Xe_2Cl and Xe_2Br are described.

Introduction

One of the most important technical problems in the development of high-energy electron beam pumped excimer lasers is the achievement of good coupling between the electron beam and the laser medium. Large mode volumes, and uniform and efficient energy deposition are needed in order to obtain high output powers. Transverse and radial excitation [1,2], provide efficient and uniform excitation. However, because of impedance effects associated with the field-emission diode, it is not practical to utilize a long cathode, and still maintain the fast rise-time necessary for excimer formation. Thus the size of the volume of the laser is limited when such excitation is used.

A longitudinal pumping scheme, where the electron-beam is injected along the direction of the optic axis, permits interaction with the laser medium over a considerable distance, and the deposition of a large fraction of the pump energy. However, this approach requires the use of a a magnetic field for beam confinement and focusing [3-5]. In this paper, we wish to describe a simple head-on longitudinal pumping design, which offers certain advantages over two alternative longitudinal pumping methods: a lambda geometry which requires bending of the electron beam into correct alignment [4,5] and an annular scheme that depends on carefully designed magnetic field profiles [6]. The only problem encountered in this head-on design is the presence of a laser reflector which must withstand the electron beam pump pulses.

The experimental arrangement, shown in Fig. 1, consists a conventional electron beam machine (Physics International Pulserad 110) with a 30 cm long reaction cell attached to front of the field emission diode. After entering the reaction cell through a 50 μm thick titanium anode foil, the e-beam pulse (1 MeV, 15 kA, 10 ns FWHF) passes directly through the first mirror of the laser optical cavity. A similar system has been described earlier [7,8] The mirror is made from a 0.3mm thick Cervit plate, which has been appropriately ground (5 m radius of curvature) and coated with a dieletric reflector (>99%). A special hard SiO_2 outer coating is applied to the dielectric stack to protect it from attack by the halogens in the reaction cell. Measurements indicate that only about 5% of the e-beam energy is lost when it passes through the Cervit mirror. Two solenoids, one placed around the diode and another around the reaction cell provide a pulsed magnetic field which confines the electron beam and keeps it from spreading while is passes through the cell. The two coils are designed to provide a uniform field along the entire path of the beam, thus eliminating field inhomogenities which may lead to losses. A Helmholtz pair at the far end of the cell diverts the beam away from the Brewster window.

The laser cavity consists of the Cervit plate inside the cell, and an external output coupler mounted in front of the Brewster window. External alignment screws permit adjustment of the internally mounted mirror. The internal mirror showed no measurable decrease in reflectivity for up to 30 shots. However, it must be mounted carefully as there is a shock wave associated with the e-beam pulse which can crack the Cervit unless it is mounted with sufficient freedom to move slightly.

* This work supported by the Office of Naval Research and the National Science Foundation.

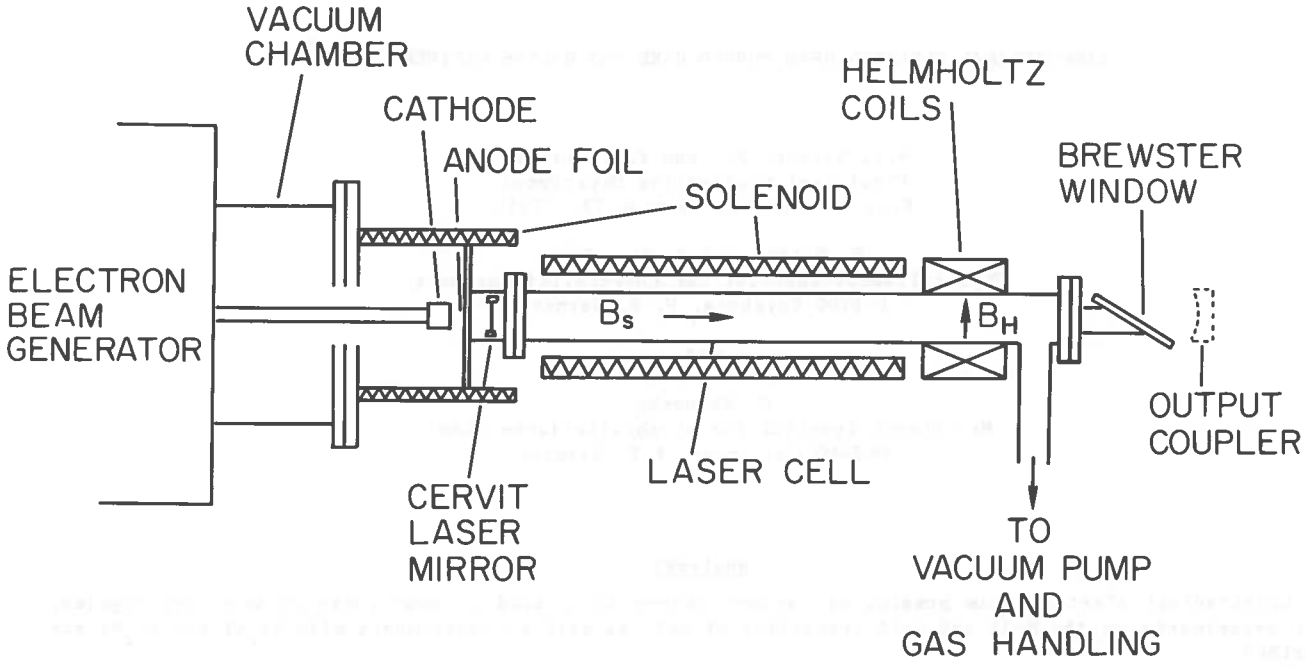

Fig. 1 Schematic of the head-on longitudinal electron beam-pumped reaction cell.

Temporal characteristics of the fluorescence and laser emission from the cell are observed with a fast vacuum photodiode, connected to a Tektronix 7912 transient digitizer. Spectral data is obtained with an optical multichannel analyzer (OMA I). All of the instrumentation is connected to a PDP 11/23 minicomputer for data manipulation and recording.

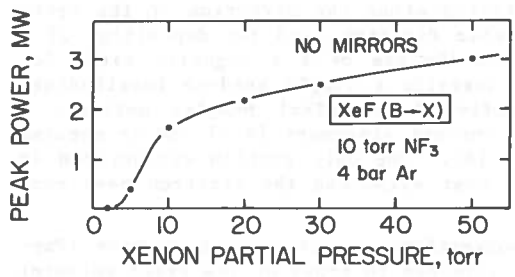

Fig. 2. a) Output power of XeF(B->X) laser as a function of xenon pressure for a mixture of 10 torr NF_3 and 4 atm argon.

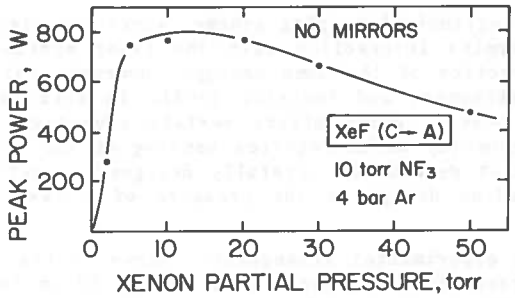

b) Variation of XeF(C->A) laser power with xenon pressure with the same gas mixture as for (a).

A variety of experiments with different rare gas-halides were performed in order to evaluate this head-on longitudinal pumping scheme. XeF, on both the narrowband B->X and wideband C->A transitions, as well as the trimers Xe_2Cl and Xe_2Br were studied. Figure 2 depicts the variation of XeF B->X and C->A emission as a function of Xe pressure in a mixture of 4 atm argon, 10 Torr NF_3, and xenon. Increasing Xe pressure increases the formation of the dimer XeF, and initially increases the emission at both the B->X and C->A wavelengths. However, as the B->X intensity grows, it becomes super-fluorescent, causing a decrease in the C->A intensity. In figure 3a), the XeF B->X and C->A fluorescence are shown, along with C->A laser emission when a mirror with 98% reflectivity from 475 to 525 nm is inserted into the laser cell. Under lasing conditions, the spectrum narrows substantially, along with a factor of 20 increase in output intensity. In the absence of mirrors, the B->X emission becomes super-fluorescent, and exceeds the C->A emission, as shown in Fig. 3b).

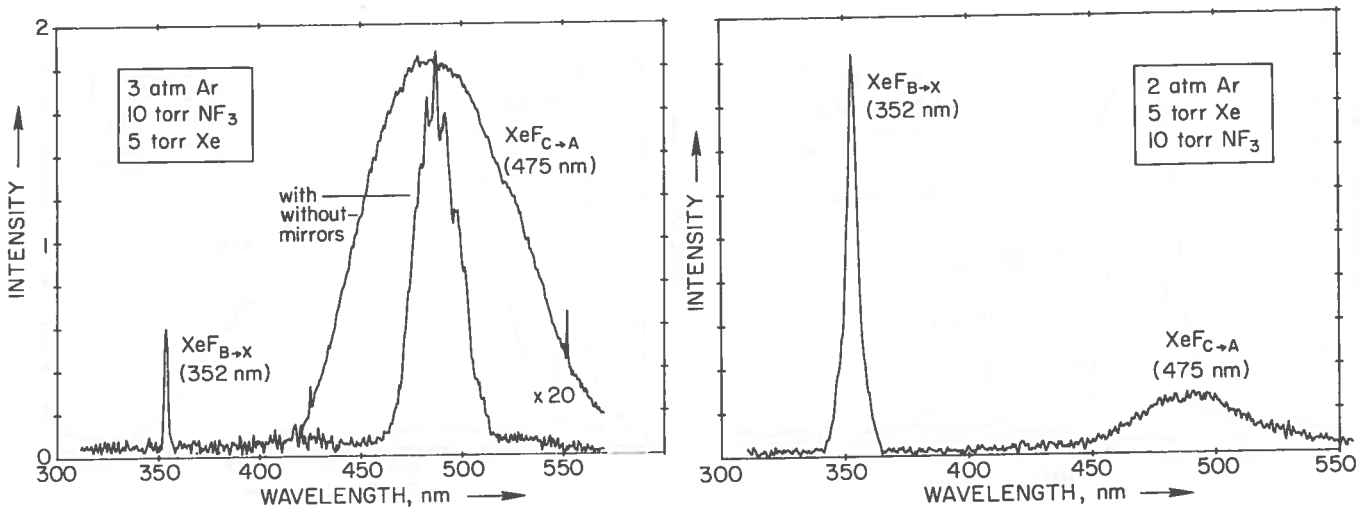

Fig. 3. Spectral characteristics of XeF* fluorescence and laser output for the blue-green C->A emission at 475 nm (a) and spectral characteristics from super-fluorescent XeF(B->X) emission at 352 nm (b).

The quenching behavior of NF_3 for both the XeF(B) and XeF(C) states is depicted in Fig. 4. For argon buffer gas pressures of 4 atm, there is strong mixing of the B and C states through collisional relaxation. Thus, when either one, or both of these levels are depopulated by nonradiative collisions, the density of both decreases. As a result, the intensity from both transitions falls off when the concentration of the halogen donor NF_3 is increased beyond an optimum value of about 8 Torr. Argon quenching, shown in Fig. 5 is not severe. The primary reason for the decrease in output power with greater than 4 atm of argon is due to increased stopping power of the argon buffer, which prevents full penetration of the cell by the electron beam. Calorimetric measurements indicate an 80% decrease in the electron beam energy at the far end of the cell when the argon buffer gas pressure is increased from 0.5 atm to 4 atm. The temporal characteristics for the XeF(B) and XeF(C) fluorescence and laser emission are shown in Fig. 6. The maximum of XeF(B) emission occurs first, indicating direct production of the B-state. The C-state is somewhat delayed since its population results mainly via collisions from the B-state. The maximum of the XeF(C) laser occurs ~ 40 ns after the B->X laser pulse due to the long cavity build-up time of this low gain transition.

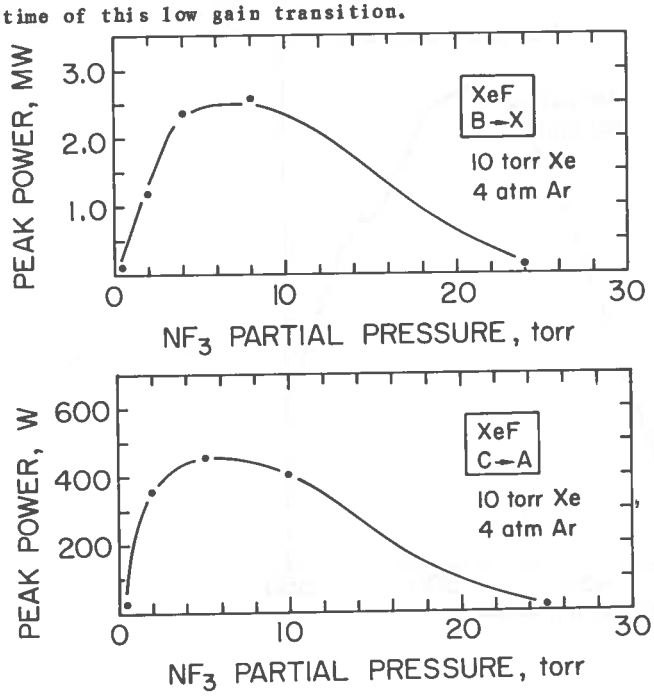

Fig. 4. Variation of XeF(B->X) (a) and C->A (b) emission as a function of the NF_3 pressure.

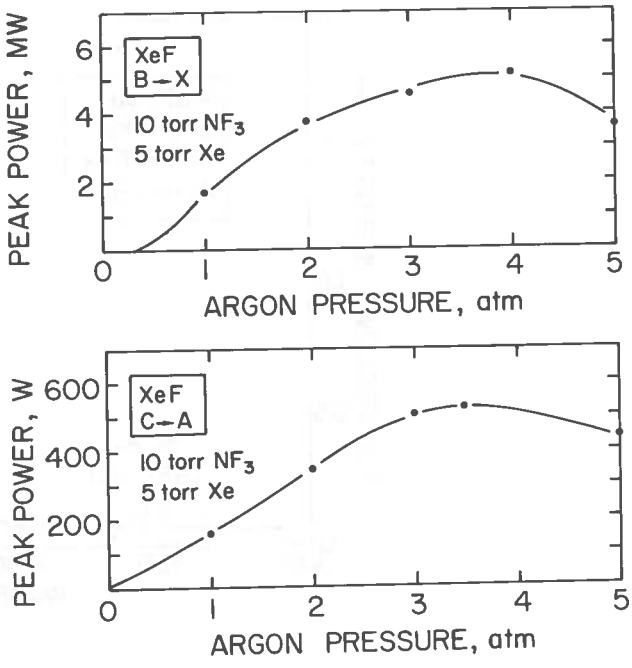

Fig. 5. Variation of XeF(B->X) (a) and C->A (b) laser emission as a function of argon partial pressure.

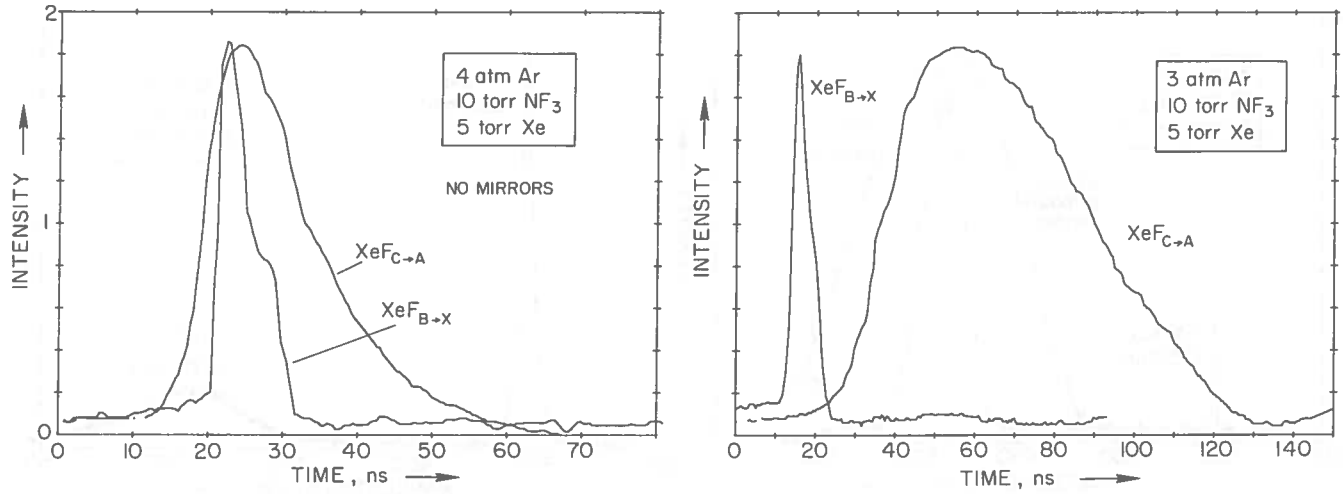

Fig. 6. Normalized temporal characteristics of XeF(B) and XeF(C) emission without resonator (a) and with resonator (b).

In an effort to reduce the stimulated emission of the B->X transition, we tried to introduce a UV absorbing gas into the rare gas-halide mixture. Figure 7 shows the fluorescence spectra, with a mixture of 2 atm Ar, 5 torr Xe, 10 torr NF_3, and 15 torr of BF_3. BF_3 has a very strong absorption in the UV, and its effect on the B->X emission is evident. Unfortunately, quenching of both the B and C states of XeF by BF_3 is strong. This can be seen in Figure 8, which is a plot of the normalized C->A and B->X intensity as a function of BF_3 partial pressure. The addition of BF_3 severly inhibits the B->X XeF emission, witn almost complete removal at pressures greater than 4 Torr. However, the C->A emission is also quenched, but not as severely. There is still some C->A emission with up to 15 Torr of BF_3 in the gas mixture. However, the quenching of the C state is quite strong, and no lasing of XeF C->A was achieved with gas mixtures containing BF_3.

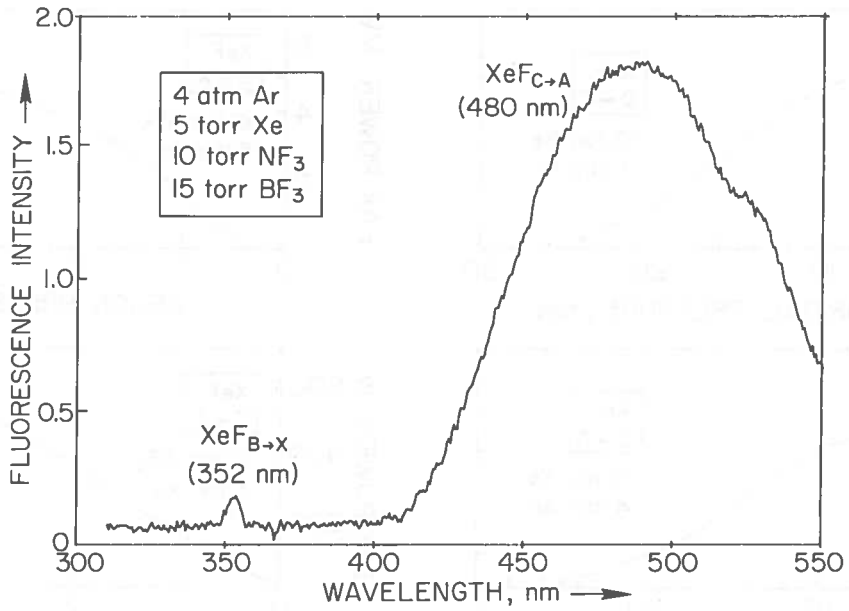

Fig. 7. XeF fluorescence spectrum for a mixture of 4 atm Ar, 5 Torr Xe, 10 Torr of NF_3 and 15 Torr of BF_3.

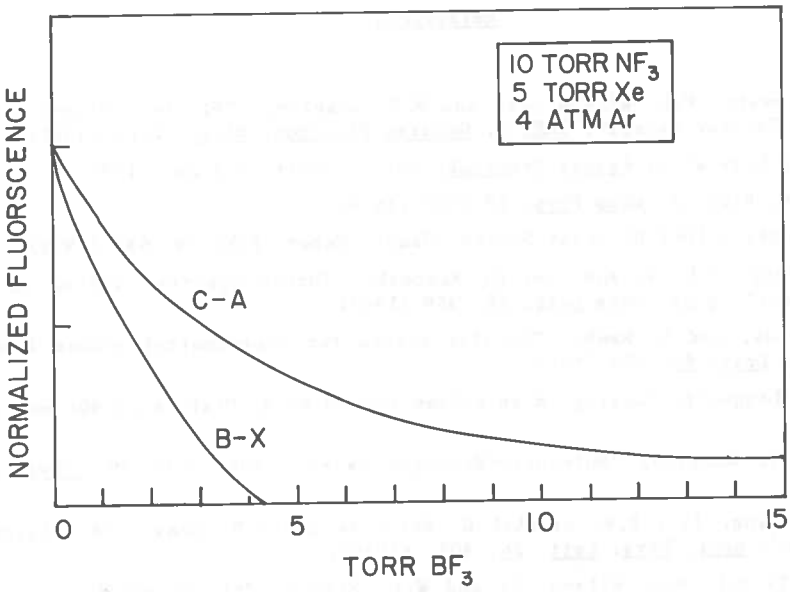

Fig. 8. Normalized B->X and C->A fluorescence emission as a function of BF_3 partial pressure.

Studies were also made of some triatomic excimers in this head-on longitudinal pumping configuration. The trimer Xe_2Cl [9] was one of those which was investigated. Figure 9 depicts some of the operating paramters for this laser. The variation in relative output power has a function of the magnetic field used for confinement of the electron beam is shown in Fig. 9a. A magnetic field of about 5 kilogauss with 3 atm Ar pressure resulted in optimum Xe_2Cl^* emission. Other paramters such as gas composition and the addition of nitrogen to reduce transient absorbers [10] were optimized at about the same values as determined in transverse electron beam pumping experiments. However, Xe_2Cl^* output power was not significantly increased in such a longitudinal cell as compared to a transverse cell. Studies were also made with the triatomic excimer Xe_2Br [11], but no evidence of laser action could be observed.

In summary, a new head-on electron beam pumping scheme has been described which permits convenient longitudinal excitation of excimer laser mixtures. Significant output powers magawatt on both the B->X and C-A transitions of XeF were observed. The primary factor limiting further improvement in the broadband blue-green C->A emission is competition from the B->X transition which becomes super-fluorescent under intense excitation conditions. The addition of BF_3 to the laser mixture to act as a selective UV absorber proved unsuccessful due to the strong quenching behavior of that molecule.

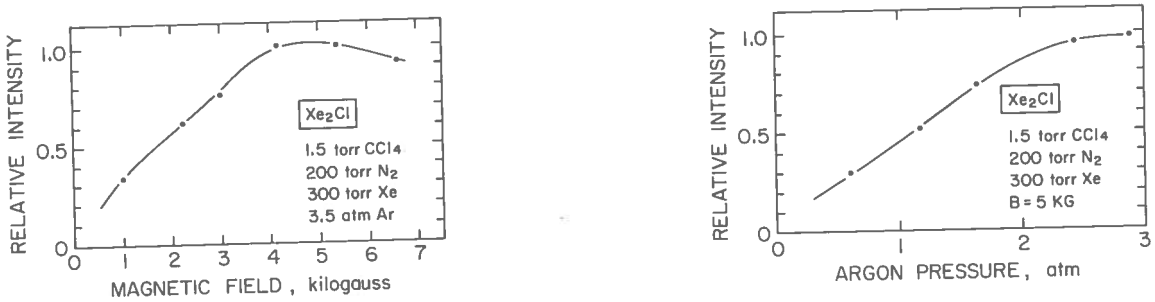

Fig. 9. Xe_2Cl emission as a function of axial confinment magnetic field (a) and as a function of argon partial pressure (b).

References

1. F.K. Tittel, G. Marowsky, W.L. Wilson, Jr. and M.C. Smayling, "Electron Beam-Pumped Broadband Diatomic and Triatomic Excimer Lasers", IEEE J. Quantum Electron. QE-17, 2268 (1981).

2. J.J. Ewing, "Excimer Lasers" in Lasers Handbook, vol. 3, North Holland, 1979.

3. J. R. Woodworth, J.K. Rice, J. Chem Phys, 69 2500 (1978).

4. R. A. Klein, λ-3 Sandia's 100J HF Laser System, Sandia Report SAND 79-1659 (1979)

5. J. Liegel, F.K. Tittel, W.L. Wilson, and G. Marowsky, "Broad Spectral Tuning of an Electron Beam Pumped XeF(C->A) Laser", Appl. Phys Lett. 39, 369 (1981).

6. Y. Kawamura, K. Toyoda, and S. Namba, "Annular e-beam for Longitudinal e-beam Pumped High Pressure Lasers", Appl. Phys. Lett. 40, 924 (1982).

7. R. Sauerbrey and H. Langhoff, "Lasing in an e-beam Pumped Ar-N_2 Mixture at 406 nm ", Appl. Phys. 22, 399 (1980).

8. R.W. Dreyfus and R.T. Hodgson, "Molecular-Hydrogen Laser: 1098-1613 Å", Phys. Rev. A 22, 2535 (1979).

9. F.K. Tittel, W.L. Wilson, Jr., R.E. Stickel G. Marowsky and W.E. Ernst, "A Triatomic Xe_2Cl Excimer Laser in the Visible", Appl. Phys. Lett. 36, 405, (1980).

10. R. Sauerbrey, F.K. Tittel, W.L. Wilson, Jr and W.L. Nighan, "Effect of Nitrogen on XeF(C->A) and Xe_2Cl Laser Performance", IEEE. J. Quantum Elecron. QE-18 1336 (1982).

11. W.L. Wilson, Jr., R.A. Williams, R. Sauerbrey, F.K. Tittel and G. Marowsky, "Formation and Quenching Kinetics of Electron Beam Excited Xe_2Br", J. Chem Phys., 77, 1830 (1982), also Appl. Phys. J. B28, 127 (1982).